

Improved Electric Properties of Degraded Liquid Crystal Using Metal–Organic Frameworks

This content has been downloaded from IOPscience. Please scroll down to see the full text.

2013 Appl. Phys. Express 6 121701

(<http://iopscience.iop.org/1882-0786/6/12/121701>)

View [the table of contents for this issue](#), or go to the [journal homepage](#) for more

Download details:

IP Address: 140.113.38.11

This content was downloaded on 28/04/2014 at 23:52

Please note that [terms and conditions apply](#).

Improved Electric Properties of Degraded Liquid Crystal Using Metal–Organic Frameworks

Cheng-Ting Huang¹, Kun-Ting Liao¹, Chia-Her Lin^{2,3}, Jy-Shan Hsu^{1,2,*}, and Wei Lee^{1,2,4*}

¹Department of Physics, Chung Yuan Christian University, Chungli 32023, Taiwan

²Center for Nanotechnology, Chung Yuan Christian University, Chungli 32023, Taiwan

³Department of Chemistry, Chung Yuan Christian University, Chungli 32023, Taiwan

⁴Institute of Imaging and Biomedical Photonics, College of Photonics, National Chiao Tung University, Tainan 71150, Taiwan

E-mail: jy_shan@cycu.edu.tw; wlee@nctu.edu.tw

Received September 15, 2013; accepted October 28, 2013; published online November 18, 2013

A series of experiments are conducted to examine the purification effect on degraded liquid crystal (LC) by soaking porous metal–organic frameworks in the LC material. The results indicate that the electric properties of the degraded LC are dramatically improved due to the adsorption and removal of moisture and impurity ions, most likely originating from the atmosphere. This investigation leads to the advancement in the feasible recycling of deteriorated LC materials, including LC leftovers from flat-panel production lines, with a simple and cost-effective treatment method.

© 2013 The Japan Society of Applied Physics

Liquid crystal display (LCD) technology has been successfully applied to many commercial products such as mobile, projector, and flat-panel devices. With the technology advancing fast and environmental issues being of intense concern, the LCD is now demanded to realize low energy consumption, high image quality, high electrooptical performance, and eco-friendly manufacturing processes. Along this line, unavoidable impurity ions in LC cells often cause serious problems such as high operation voltage, low voltage holding ratio, slow switching response, grey-level shift, image sticking, and image flickering.^{1–4} To reduce the ion concentration and suppress the ion transport, various methods have been suggested to ameliorate the LCD performance. For example, the deposition technique of SiO_x alignment films can generate less impurity ions on the alignment-layer surface than rubbed polyimide,⁵ and a 5° SiO_x film results in a low ion concentration in the LC cell via ion adsorption and capture.⁶ Moreover, doping trace amounts of multiwalled carbon nanotubes,⁷ anatase TiO₂ nanoparticles,⁸ and montmorillonite clay platelets⁹ into LCs has been confirmed to mitigate the ionic effect. In addition, our previous work indicates that natural degeneration of LC in sealed bottles can primarily be attributable to the permeation of atmospheric water vapor from air.¹⁰ Water molecules present in LC can be dissociated into hydrogen cation and hydroxyl anion, yielding a considerable amount of impurity ions to enhance the ionic effect and, thereby, worsening the electrooptical performance. It has been established that the coordination polymer M2B as a desiccant can restore the electric resistivity of a degraded LC by absorbing and removing moisture from the mesogenic material. The “regenerated” LC exhibited much lower ion concentration than did the untreated counterpart.¹⁰

This study aims to investigate the effect of metal–organic frameworks (MOFs) as powerful purifying agents on restoring the electric properties of degraded, or more precisely, contaminated LC. MOFs^{11–13} are a new class of porous substances constructed from metal ions clusters connected by multifunctional organic linkers, producing three-dimensional networks with large inner surface areas and pore volumes. Owing to their large specific surface areas as well as total pore volumes, MOFs are promising materials for many applications such as gas storage, catalysis, gas separation, and water adsorption.¹⁴ In this work, we compared water-sorption kinetics of various desiccants including

MOFs. In order to inspect the material and device properties of degraded LC after purification with MOFs via soaking, we measured the DC voltage-dependent capacitance (*C*–*V*) curves,¹⁵ calculated ion concentrations by low-frequency dielectric spectroscopy,¹⁶ and performed inductively coupled plasma mass spectrometry (ICP-MS) on a fresh LC counterpart and degraded LC samples prior to and after treatments with MOFs. The effects of soaking MOFs and stirring during the treatment process were examined by voltage holding ratio (VHR) measurements.

The LC material investigated is designated G1 (with dielectric anisotropy $\Delta\epsilon = 7.9$ and clearing point 120 °C), a TFT-grade LC used in the current display market. The resistivity of brand-new G1 (G1N) was $\sim 10^{13} \Omega\text{-cm}$, whereas that of G1 received as a leftover from the panel production line (G1L) was $\sim 10^{12} \Omega\text{-cm}$. MOFs used in this study included (1) HKUST-1,¹⁷ a microporous material with the formula [Cu₃(BTC)₂(H₂O)₃] (where BTC is benzene-1,3,5-tricarboxylate); (2) MIL-100(Cr),¹⁸ a mesoporous chromium trimesate of chemical composition [Cr₃F(H₂O)₃O(BTC)₂] $\cdot n$ H₂O (where $n \sim 28$); (3) MIL-101(Cr),¹⁹ a mesoporous chromium terephthalate with the formula [Cr₃F(H₂O)O(BDC)₃] $\cdot n$ H₂O (where BDC is benzene dicarboxylate and $n \sim 25$). These MOFs were synthesized in the Solid-State Chemistry Laboratory at Chung Yuan Christian University. HKUST-1 has open channels in three directions whereas both MIL-100(Cr) and MIL-101(Cr) have cage structures to exhibit porous properties. All the three MOFs possess open structures with pore windows about 1.0 to 1.6 nm in size as well as large surface areas from 1500 to 4000 m²/g. Meanwhile, all Cu atoms in HKUST-1 and two-thirds of Cr atoms in either MIL-100 species lined up on the pore walls will become active to capture water molecules when they are used for purification treatment. Fundamentally, these MOFs display water physisorption and chemisorption properties due to the highly porous space and unsaturated metal sites. The adsorption of water molecules occurs around the hydrophilic metal ion clusters and vacant metal sites at low humidity. The water adsorption also correlates closely with the available pore volume within hydrophobic pores containing organic ligands at high humidity. In general, inorganic and organic pollutants can well be trapped within these porous MOFs. The fact that a MOF can serve as an active agent for recycling of contaminated LCs stems presumably from its

high porosity. The MOFs carefully chosen for this investigation have distinguished specific surface areas and total pore volumes, enabling effective adsorption of water molecules and impurity ions in degraded LCs. Additionally, the MOFs we used are characterized by their unsaturated metal sites or active sites to further promote the sorption capacity. These highly porous MOF structures with unsaturated metal sites and originally nanoporous channels or volumes can enormously take up water and impurity ions in LC leftovers, making their purifying capability superior to that of typical nanoporous materials such as silicates or ordinary MOFs.

To take full advantage of the high adsorption capacity, the moisture in MOFs must first be removed. Each MOF material, heated beforehand at 150 °C for about 12 h in a vacuum oven and then cooled to room temperature, was soaked in a sealed G1L vial for 24 h if not specified. When the treatment was completed, “purified” G1L was drawn out of the vial through a filter and then filled into 6.7 ± 0.1 - μm -thick empty antiparallel planar-alignment cells coated with indium–tin-oxide electrodes.

The ion content can be acquired by fitting the real-part (ϵ') and imaginary-part (ϵ'') dielectric constant ϵ^* inferred from the low-frequency complex dielectric function according to¹⁶⁾

$$\epsilon'(f) = \frac{nq^2 D^{3/2}}{\pi^{3/2} \epsilon_0 d k_B T} f^{-3/2} + \epsilon'_b, \quad (1)$$

$$\epsilon''(f) = \frac{nq^2 D}{\pi \epsilon_0 k_B T} f^{-1}, \quad (2)$$

where n is the ionic concentration, q is the electric charge, D is the diffusion constant, f is the frequency, ϵ_0 is the dielectric permittivity in vacuum, d is the cell gap, k_B is the Boltzmann constant, T is the absolute temperature, and ϵ'_b is the intrinsic dielectric constant of the LC bulk. The contribution of the electric double layers may take place at frequencies under 1 Hz and the space-charge polarization occurs below 10^3 Hz in the dielectric loss (ϵ'') spectrum.²⁰⁾ The frequency-dependent complex dielectric constant $\epsilon^* = \epsilon' - i\epsilon''$ was measured with an LCR meter (Hioki 3522-50). The probe voltage was $0.5 V_{\text{rms}}$, which was lower than the threshold voltage of the LC in the sinusoidal waveform.

According to a previous study,²¹⁾ if a LC contains more ionic impurities, then the VHR of the LC cell will be lower. Critically, the VHR is a reliability parameter for the frame-memory technique widely adopted in active-matrix devices; a lower VHR often corresponds to the decrease in contrast, nonuniformity of brightness, and even image sticking. The VHR can simply be defined as²²⁾

$$\text{VHR} = \frac{A_t}{A_i} \times 100 (\%), \quad (3)$$

where A_t and A_i represent the areas below the actual and ideal voltage curves during a single pulse time, respectively. In this study, the pulse width of the scan line was $15.6 \mu\text{s}$ at 60 Hz, and the data line was a 5 V square-wave signal with a pulse time of 16.67 ms.

Figure 1 shows the time-dependent weight gains of various dried MOFs compared with those of a commercial drying agent (silica gel) and M2B used in our previous work.¹⁰⁾ Each uncovered Petri dish containing each kind of 1 g of agent was placed in a closed dry cabinet containing a

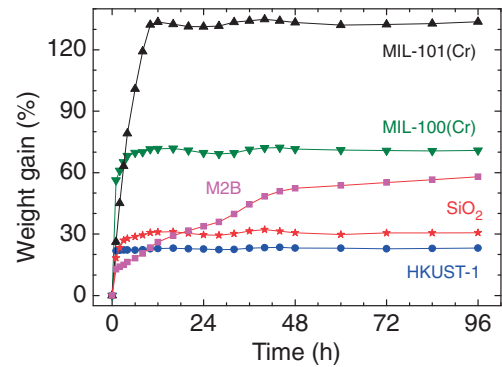


Fig. 1. Time-dependent weight gain of various drying agents.

beaker of water. The temperature and relative humidity in the cabinet were 26 ± 1 °C and $50 \pm 5\%$, respectively. The water adsorption capacity was determined by the weight gain (W_{gain}) according to

$$W_{\text{gain}} = \frac{W_{\text{total}} - W_{\text{dried}}}{W_{\text{dried}}} \times 100 (\%), \quad (4)$$

where W_{total} and W_{dried} are the total and dry weights of the test materials, respectively. The water adsorption capacity rose steeply within 12 h and saturated after 24 h for all desiccants except M2B, implying that the MOFs are more efficient than M2B. The saturated weight gains were higher than 60% for all MOFs except HKUST-1. With an extremely high water-adsorption capacity of over 130%, MIL-101(Cr) outperformed the other desiccants.

Figure 2 shows the DC C - V curves of various cells of untreated and treated LC samples. Figures 2(a) and 2(e) depict C - V curves of G1L and G1N samples, respectively. Clearly, the hysteresis width between the voltage-up and voltage-down processes of the G1L cell is larger than that of G1N, suggesting that the internal electric field established by the impurity ions in G1L was stronger. Therefore, we speculated that G1L had more impurity ions than G1N. Figures 2(b)–2(d) reveal C - V properties of G1L treated with 1 wt % HKUST-1, MIL-100(Cr), and MIL-101(Cr), respectively. Apparently, all the treated G1L samples exhibited narrower hysteresis widths than did the untreated one, and G1L treated with MIL-101(Cr) showed the narrowest hysteresis width. These findings indicated that all MOFs can effectively abate the internal, counteracting electric field and improve the electric properties of the LC cells and, noticeably, that MIL-101(Cr) is most effective in terms of removal of impurity ions. A closer comparison between Figs. 1 and 2 permits one to presume that the purifying ability of a MOF (for contaminated LC) is strongly correlated with its water adsorption capacity. Further examination with a Karl Fischer titrator for water content determination is preferred to confirm the effectiveness of treatment with a MOF sorbent.

The ion contents of G1N and untreated G1L, deduced via Eqs. (1) and (2), were 9.1×10^{-2} and 11 nC/cm^3 , respectively. Figure 3 shows the mobile ion concentration in G1L treated with 0.1, 0.5, and 1.0 wt % MOFs. Manifestly, the ion content of the treated G1L dropped rapidly when the MOF concentration was 0.1 wt %; it decreased further with increasing MOF concentration. In the case of 1.0 wt %

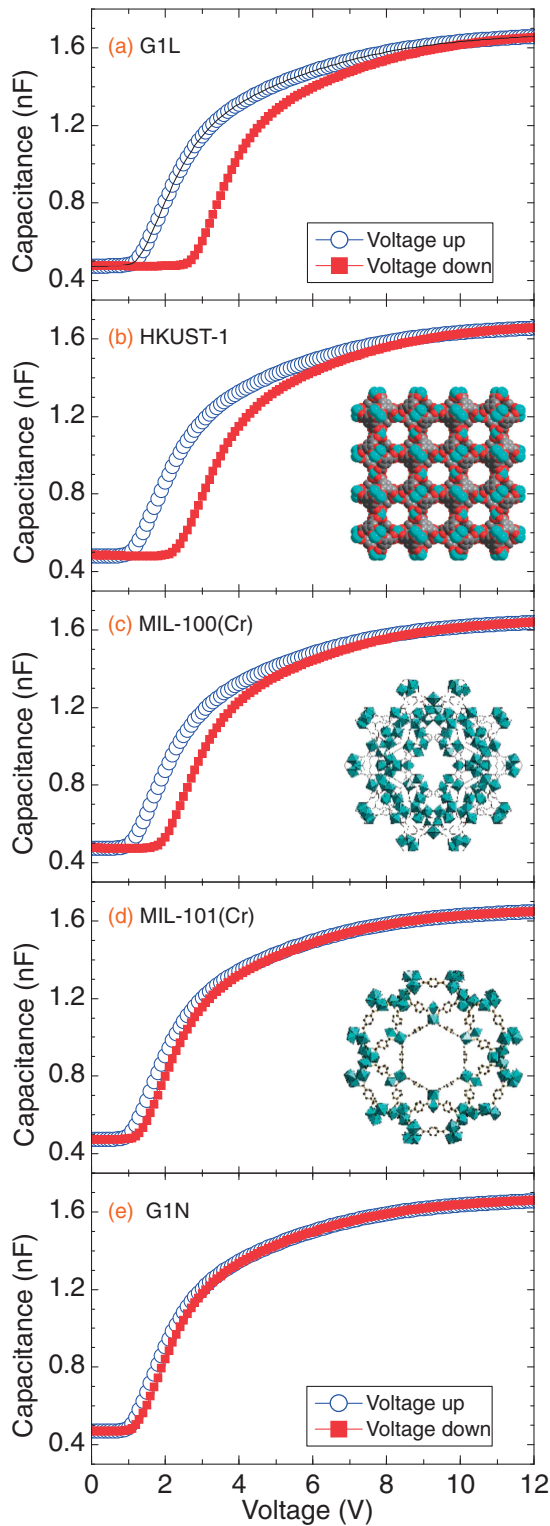


Fig. 2. DC C - V of (a) untreated G1L, G1L treated with (b) HKUST-1, (c) MIL-100(Cr), and (d) MIL-101(Cr) at a concentration of 1 wt % for 24 h of soaking, and (e) G1N as received.

MIL-101(Cr) for treatment, the ion concentration was 0.16 nC/cm^3 , which was the lowest. In contrast, for 1 wt % HKUST-1 treatment, the ion concentration (of 0.31 nC/cm^3) was two times higher. Obviously, the ion removal efficiency is positively related with the MOF concentration. We speculate from both Figs. 2 and 3 that MOFs can diminish the ion effect by reducing the impurity ion concentration in G1L.

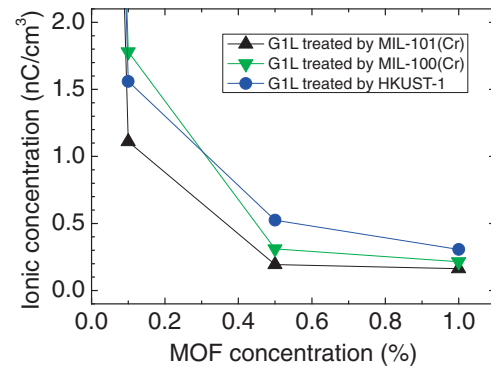


Fig. 3. Mobile ion content of MOF-treated G1L as a function of MOF concentration for 24 h of treatment.

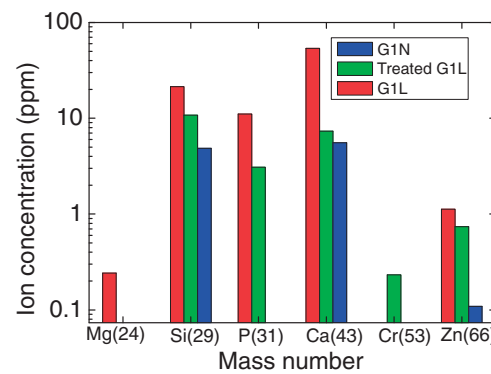


Fig. 4. Element abundance of primary impurities in G1N, G1L, and G1L treated with 1.5 wt % MIL-101(Cr) for 24 h.

Obtained from the ICP-MS (Perkin Elmer SCIEX ELAN 5000) data, Fig. 4 shows the element abundance in G1N, G1L, and G1L treated with 1.5 wt % MIL-101(Cr). Note that the highest concentrations of impurities excluding Cr were found in G1L. Figure 4 infers that MIL-101(Cr) is capable of purifying contaminated LC by not only absorbing moisture but also capturing element impurities. We believe that the contaminants found in G1L originated from airborne particles when the LC was in contact with air. A drawback of the use of MIL-101(Cr) for LC regeneration is the presence of a trace of Cr in the treated G1L sample, which was most likely released from the MOF itself.

Figure 5 depicts VHR of G1N and G1L treated with MIL-101(Cr). Perceptibly, VHR of treated G1L increased with increasing soaking time, rising rapidly within 24 h and slowly saturated to the value of G1N. Figures 1–5 allow one to conclude that the contamination in G1L was caused by the permeation of moisture and the particulates from air into G1L. The result as shown in Fig. 6 is in line with the common understanding that stirring a mixture accelerates chemical reactions. Here, the stirring process promoted the purification efficiency, cutting the treatment time by at least half compared with that without stirring.

In summary, porous MOF materials are composed of metal ions or clusters of metal ions coordinated to organic ligands. The choice of metal and linker has significant effects on the structure and properties of a MOF. The MOFs employed in this work, including HKUST-1, MIL-100(Cr),

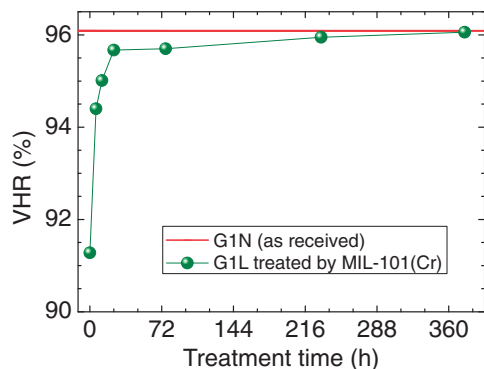


Fig. 5. VHR of LC cells consisting of G1N and G1L treated with 1 wt % MIL-101(Cr) at various treatment durations.

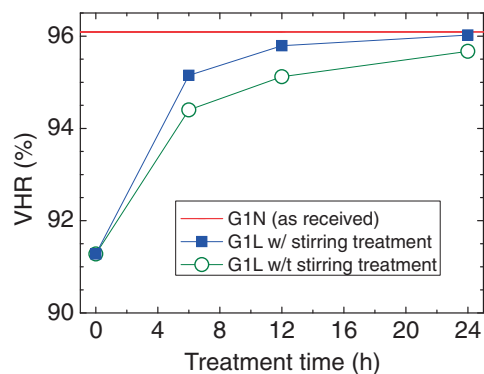


Fig. 6. VHR of LC cells containing G1N and G1L treated with 1 wt % MIL-101(Cr) with and without magnetic stirring at 500rpm during the treatment.

and MIL-101(Cr), all possess high porosities as well as large specific surface areas and are well known for excellent thermal and moisture stability. They have been well documented to hold promise for applications as powerful desiccants against atmospheric moisture.^{14,23} We have demonstrated in this study that MOFs, a new class of porous material, can be utilized to promote the electrically resistive properties of degraded or contaminated TFT-grade LC via the soaking treatment. Both MIL-100(Cr) and MIL-101(Cr) showed a higher water adsorption capacity than silica gel. As effective adsorbent, a MOF with a higher water adsorption capacity exhibited stronger purification ability for the regeneration of LC. The ICP-MS data delineated that MIL-101(Cr) can also remarkably reduce the abundance of various contaminants in G1L. Increasing both the MOF concentration and soaking time for treatment can enhance the effect of purification. The VHR data further showed that stirring enables a more sufficient treatment. Our findings are of great practical importance for the design of green

manufacturing technology for the current \$100B LCD market, reducing the amount of outcast materials of LC and the like.

Using MOFs with unsaturated metal sites (or active sites) in addition to high porosity and specific surface area, we have manifested a novel approach to purifying contaminated LCs from a leftover. Other MOF candidates having similar structures are MIL-100 series consisting of metal (III) species such as MIL-100(Fe), MIL-100(Al), MIL-100(V), MIL-100(In), and MIL-100(Mn), which can be examined for their potential applications in recycling of LCs. To further improve the purifying performance, one may consider functionalized MOF coordination structures with surface modification by additional functional groups such as amino ($-\text{NH}_2$), sulfone ($-\text{SO}_3$), and phosphate ($-\text{PO}_3$) groups to enhance the overall adsorption efficacy. Research along this line is underway in this laboratory.

Acknowledgments We thank WINTEK Corporation for providing LC samples (both G1N and G1L). This ongoing research is financially supported by the National Science Council of Taiwan, Republic of China, under Grant No. NSC 100-2632-M-033-001-MY3.

- 1) S. H. Perlmuter, D. Doroski, and G. Moddel: *Appl. Phys. Lett.* **69** (1996) 1182.
- 2) C. Colpaert, B. Maximus, and A. De Meyere: *Liq. Cryst.* **21** (1996) 133.
- 3) V. A. Tsvetkov and O. V. Tsvetkov: *Mol. Cryst. Liq. Cryst.* **368** (2001) 625.
- 4) L. O. Palomares, J. A. Reyes, and G. Barbero: *Phys. Lett.* **A333** (2004) 157.
- 5) J. L. Janning: *Appl. Phys. Lett.* **21** (1972) 173.
- 6) Y. Huang, P. J. Bos, and A. Bhowmik: *J. Appl. Phys.* **108** (2010) 064502.
- 7) H.-Y. Chen and W. Lee: *Appl. Phys. Lett.* **88** (2006) 222105.
- 8) C.-Y. Tang, S.-M. Huang, and W. Lee: *J. Phys. D* **44** (2011) 355102.
- 9) H.-H. Liu and W. Lee: *Appl. Phys. Lett.* **97** (2010) 023510.
- 10) W. Lee, C.-T. Wang, and C.-H. Lin: *Displays* **31** (2010) 160.
- 11) S. Kaskel, F. Schüth, K. S. W. Sing, and J. Weitkamp: *Handbook of Porous Solids* (Wiley-VCH, Weinheim, 2002).
- 12) O. M. Yaghi, H. Li, C. Davis, D. Richardson, and T. L. Groy: *Acc. Chem. Res.* **31** (1998) 474.
- 13) M. Eddaoudi, J. Kim, N. Rosi, D. Vodak, J. Wachter, M. O'Keefe, and O. M. Yaghi: *Science* **295** (2002) 469.
- 14) P. Küsgens, M. Rose, I. Senkovska, H. Fröde, A. Henschel, S. Siegle, and S. Kaskel: *Microporous Mesoporous Mater.* **120** (2009) 325.
- 15) W. Lee, C.-Y. Wang, and Y.-C. Shih: *Appl. Phys. Lett.* **85** (2004) 513.
- 16) G. Barbero and A. L. Alexe-Ionescu: *Liq. Cryst.* **32** (2005) 943.
- 17) S. S.-Y. Chui, S. M.-F. Lo, and J. P. H. Charmant, A. G. Orepn, and I. D. Williams: *Science* **283** (1999) 1148.
- 18) G. Férey, C. Serre, C. Mellot-Draznieks, F. Millange, S. Surblé, J. Dutour, and I. Margiolaki: *Angew. Chem., Int. Ed.* **116** (2004) 6456.
- 19) G. Férey, C. Mellot-Draznieks, C. Serre, F. Millange, J. Dutour, S. Surblé, and I. Margiolaki: *Science* **309** (2005) 2040.
- 20) A. Sawada, K. Tarumi, and S. Naemura: *Jpn. J. Appl. Phys.* **38** (1999) 1418.
- 21) T. Nakanishi, T. Takahashi, H. Mada, and S. Saito: *Jpn. J. Appl. Phys.* **41** (2002) 3752.
- 22) H. Seiberle and M. Schadt: *Mol. Cryst. Liq. Cryst.* **239** (1994) 229.
- 23) S. K. Henninger, F. Jeremias, H. Kummer, and C. Janiak: *Eur. J. Inorg. Chem.* **2012** (2012) 2625.